

Pore water evolution in oilfield sandstones: constraints from oxygen isotope microanalyses of quartz cement

Ann M.E. Marchand^{a,*}, Calum I. Macaulay^b,
R. Stuart Haszeldine^a, Anthony E. Fallick^c

^aDepartment of Geology and Geophysics, University of Edinburgh, Edinburgh EH9 3JW, Scotland, UK

^bShell International Exploration and Production, Houston, TX 77025, USA

^cScottish Universities Environmental Research Centre, East Kilbride G75 0QF, Scotland, UK

Received 10 December 2001; accepted 5 June 2002

Abstract

Oxygen isotope microanalyses of authigenic quartz, in combination with temperatures of quartz precipitation constrained by fluid inclusion microthermometry and burial history modelling, are employed to trace the origin and evolution of pore waters in three distinct reservoirs of the Brae Formation in the Miller and Kingfisher Fields (North Sea). Oxygen isotope ratios of quartz cements were measured in situ in nine sandstone thin sections with a Cameca ims-4f ion microprobe. In conjunction with quartz cement paragenesis in the reservoirs, constrained from textural and cathodoluminescence (CL) microscopy studies, pore water evolution was reconstructed from the time of deposition of the sandstones in the Upper Jurassic until the present.

CL photomicrographs of quartz overgrowths in the Brae Formation sandstones show three cement zones (A, B and C) which can be related to different oxygen isotope compositions: (1) the earliest, and thinnest, zone A (homogeneous CL pattern with probable $\delta^{18}\text{O}$ values between +23‰ and +26‰—direct measurements were not possible) precipitated in the sandstones at temperatures <60 °C; (2) the second zone B (complex CL pattern and directly measured $\delta^{18}\text{O}$ values between +15‰ and +18‰) precipitated in the sandstones most likely between 70 and 90 °C; (3) the third zone C (homogeneous CL pattern and directly measured $\delta^{18}\text{O}$ values between +16‰ and +22‰) precipitated in the sandstones most likely at temperatures >90 °C. Calculated oxygen isotope compositions of pore waters show that zone A quartz cements, and enclosing concretionary calcite, precipitated from a meteoric-type fluid ($\sim -7\%$) during shallow burial (<1.5 km). Zone B quartz cements precipitated from fluids which evolved in composition from a meteoric-type fluid ($\delta^{18}\text{O} -7\%$) to a more ^{18}O -enriched fluid ($\delta^{18}\text{O} -4\%$) as burial continued to ~ 3.0 km. Data from zone C quartz cements are consistent with further fluid evolution from $\delta^{18}\text{O} -4\%$ to basinal-type fluids with $\delta^{18}\text{O}$ similar to the present-day formation water oxygen isotope composition (+0.6‰ at 4.0 km burial). A similar pore water evolution can be derived for all three reservoirs studied, indicating that hydrogeologic evolution was similar across sandstones of the whole Brae Formation.

The quartz cement zones observed in the Brae Formation sandstones, and the pore water history derived for the area studied, is analogous to published petrographic and pore water evolution data from the nearby Brent Group reservoirs and from reservoirs located in the Haltenbanken area on the Atlantic margin offshore Norway. Considering quartz cement is a major porosity-occluding phase in many reservoir sandstones, and because pore waters both dissolve quartz and carry the

* Corresponding author. 11514 Olympia Drive, Houston, TX 77077, USA. Tel.: +1-281-2930611.

E-mail address: anmarchand1@aol.com (A.M.E. Marchand).

dissolved silica to cementation sites, the data presented are valuable for improving the understanding and prediction of reservoir quality development in sandstones globally.

© 2002 Elsevier Science B.V. All rights reserved.

Keywords: Pore water; Quartz cement; Oxygen isotopes; Ion microprobe; Cathodoluminescence; Fluid inclusions

1. Introduction

Quartz cement is a major destroyer of porosity and an important control on reservoir quality in many deeply buried sandstone reservoirs (e.g. Bjørlykke et al., 1986; Land and Fisher, 1987; Ehrenberg, 1990). Understanding the origin and distribution of quartz cement is consequently of economic importance for reservoir quality prediction in oilfield sandstones. Quartz cementation in sandstones during burial is governed by three linked steps: (1) dissolution of a silica source, (2) silica transport in solution and (3) quartz cement precipitation. In this paper, the nature of the fluid in which silica is transported from the site of dissolution to the site of precipitation is elucidated. Our study concentrates on the Brae Formation sandstone reservoirs of the Miller and Kingfisher oilfields (North Sea) (Fig. 1). Constraining the hydrogeological regime, which operated during the geological history of the Brae Formation sandstones, can enhance the understanding of the quartz cementation process and facilitate prediction of quartz cement distributions in the reservoirs studied. The Brae Formation sandstones are Upper Jurassic submarine fan deposits presently buried to depths of 4.0 km. Porosities in the hydrocarbon reservoirs examined typically have been reduced by 5 to 15% quartz cement (Marchand et al., 2000).

Provided quartz precipitation temperatures are known, the oxygen isotope composition of the fluid from which silica was precipitated can be calculated from oxygen isotope ratios measured in quartz cement (Longstaffe, 1989). To date, oxygen isotope compositions of quartz cement reported in most papers have been determined using bulk analysis techniques (e.g. Milliken et al., 1981; Haszeldine et al., 1992; McLaughlin et al., 1996; Macaulay et al., 1997). These methods utilise chemical and physical disaggregation techniques in order to separate authigenic from detrital quartz (Lee and Savin, 1985; Brint et al., 1991). In this paper, oxygen isotope analysis of quartz cements from the Brae Formation reservoirs was

carried out by means of secondary ion mass spectrometry (SIMS). With the ion microprobe, individual quartz overgrowths, and potentially also different growth zones in the overgrowths, can be analysed in situ with a spatial resolution of $\sim 20 \mu\text{m}$ (e.g. Graham et al., 1996; Williams et al., 1997; Lyon et al., 2000; Macaulay et al., 2000). The sequence of growth of different quartz phases in the Brae Formation sandstones was constrained by means of scanning electron microscopy (SEM)-based cathodoluminescence (CL) and petrographic analyses. The measurement of the oxygen isotope ratios in each quartz growth phase, in combination with quartz precipitation temperatures independently constrained from fluid inclusion and basin modelling studies, permitted the construction of a pore water evolution model for the Brae Formation sandstones which reveals the nature of the fluids involved in quartz cementation of the reservoirs.

2. Geological setting

The Brae Formation sandstones in the Miller and Kingfisher Fields were deposited as deepwater fans along the fault-bounded western margin of the South Viking Graben (McClure and Brown, 1990). Interbedded and overlain with Kimmeridge Clay source rocks (Harms et al., 1981), the sandstones currently host a complex of oil and gas condensate reservoirs in chronostratigraphically different units (Rooksby, 1991). The oil reservoirs in the Miller and Kingfisher Fields are located in the Brae Formation Unit 2 sandstones and are presently buried to depths of around 4.0 km (Fig. 1). A structural saddle separates the oil accumulations, but preserves a communal aquifer (Fig. 1). The gas condensate reservoir in the Kingfisher Field is located in the shallower (3.8 km) Brae Formation Unit 1 sandstones (Fig. 1). This reservoir is separated from the Brae Formation Unit 2 oil reservoir by around 25 m of Kimmeridge Clay mudstones (Fig. 1).

3. Analytical methods

3.1. Fluid inclusion microthermometry and basin modelling

Minimum temperatures of quartz cementation were obtained by measuring the homogenization temper-

atures of fluid inclusions in quartz cements using a Linkam THM600 heating–cooling stage. Because the samples are from hydrocarbon reservoirs, waters within the fluid inclusions are likely to be methane bearing. Hence, it is reasonable to assume that homogenization temperatures are very similar to true trapping temperatures and do not require pressure correc-

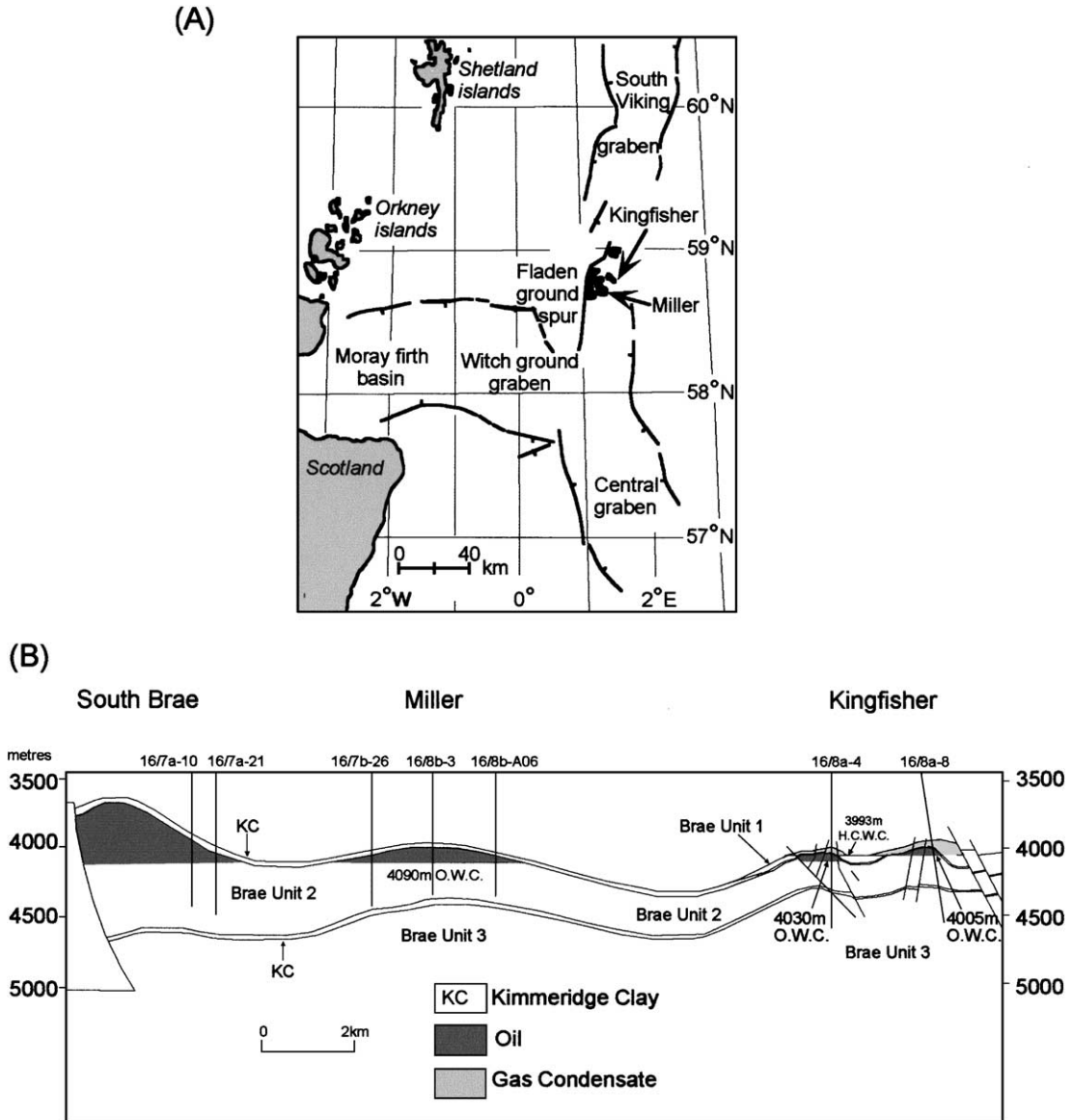


Fig. 1. (A) Location map of the Miller and Kingfisher Fields in the North Sea. (B) Structural profile across the Miller–Kingfisher Fields. The Brae Unit 2 oil reservoirs in the different fields are separated by a structural saddle but still have a communal aquifer. The gas condensate reservoir in the Kingfisher Field is located in the shallower Brae Unit 1 sands (after Marchand et al., 2001, 2002).

tion (Hanor, 1980). Polished wafers for fluid inclusion analysis were made from 24 samples from six different wells in the Miller Field and 10 samples from two different wells in the Kingfisher Field. An overview of the sample depths is provided in Table 1. The approximate time and duration of quartz cementation in the different reservoirs was constrained by combining fluid inclusion temperatures with burial and temperature history modelling of the reservoir rocks using the BasinMod™ 1D-modelling package. This program uses stratigraphic well log data, thermal conductivities and heat flow as input values. Heat flow values were derived from measured bottom-hole temperatures in wells. More details on the reconstruction of burial and temperature history in the Miller and Kingfisher Fields are provided in Marchand et al. (2001, 2002).

3.2. Oxygen isotope microanalysis

Oxygen isotope ratios in quartz cement were measured with a Cameca ims-4f ion microprobe equipped with a Charles Evans & Associates control system at the University of Edinburgh. Analyses were made with a focused (20–25 µm) primary beam of $^{133}\text{Cs}^+$ ions accelerated onto gold-coated polished thin sections. Negative high-energy (offset 350 V) secondary ions ($^{18}\text{O}^-$ and $^{16}\text{O}^-$) were accelerated and focused into a mass spectrometer where the isotopes were magnetically separated and subsequently counted with an electron multiplier. For each analysis of $^{18}\text{O}/^{16}\text{O}$ in quartz, secondary $^{18}\text{O}^-$ and $^{16}\text{O}^-$ ions were collected with total counting times of

640 and 80 s, respectively. Analytical precision on individual analyses using the SIMS technique is $\pm 1\%$ which is adequate for reservoir quality applications (Graham et al., 1996; Macaulay et al., 2000). Quartz analyses were standardised against Bogala Quartz (BOG) ($\delta^{18}\text{O}_{\text{SMOW}} = 12.3 \pm 0.3\%$; Else-heimer and Valley, 1993). The homogeneity of this standard at the scale of ion microprobe analysis was demonstrated by Graham et al. (1996).

Nine samples were selected for analysis (Table 2). Samples were made into polished thin sections (30 µm thick) and cut to circles of 1 in. diameter in order to fit into the ion microprobe sample holders. As quartz is an electrical insulator, the sections were gold-coated to prevent charge build up on the sample surface. Prior to oxygen isotope analysis, an SEM image map (in secondary electron (SE) and CL mode) was made for each thin section sample. Quartz cement CL zones suitable for analysis (>20 µm thick) were identified and marked on each sample map. The SEM SE and CL photomicrograph maps were subsequently used during the SIMS analysis session to facilitate identification of the areas of interest in the reflected light optical viewing system of the ion microprobe.

4. Quartz cementation in the Brae Formation reservoirs

4.1. Quartz cementation conditions

Quartz cementation is the main cause of porosity loss in the Brae Formation sandstone reservoirs of the

Table 1

Sampled depth intervals of rocks used for fluid inclusion and/or SIMS analysis in this study and average (\pm standard deviation) mineralogical compositions for each interval

Field	Reservoir	Well	Sample depth (m)	Detrital quartz (%)	Feldspar (%)	Rock fragments (%)	Detrital clay (%)	Others (%)		
Miller	Brae Unit 2	7b-A03	4022–4070	88.2 \pm 3.7	2.9 \pm 0.7	3.2 \pm 1.6	3.5 \pm 2.3	2.2 \pm 2.6		
		8b-3	3989–4116	86.3 \pm 3.5	3.0 \pm 1.4	4.8 \pm 1.8	2.2 \pm 0.7	3.7 \pm 2.1		
		7b-24	4045–4113	87.5 \pm 2.6	3.9 \pm 0.9	2.9 \pm 1.6	2.8 \pm 1.2	3.0 \pm 1.7		
		8b-5	4086–4145	87.1 \pm 0.3	1.5 \pm 0.6	5.4 \pm 0.7	3.2 \pm 2.9	2.8 \pm 1.7		
		8b-A06	4065–4112	89.6 \pm 1.9	2.1 \pm 0.7	4.7 \pm 1.5	1.8 \pm 1.0	1.8 \pm 0.7		
		7b-26	4101–4186	89.0 \pm 2.5	2.6 \pm 0.6	3.2 \pm 0.7	2.5 \pm 0.5	2.7 \pm 0.9		
		7b-28	4080–4085	87.3 \pm 5.2	3.1 \pm 1.8	2.1 \pm 1.0	2.4 \pm 0.9	5.1 \pm 3.1		
		8b-A10	4094–4105	84.8 \pm 4.0	3.0 \pm 0.3	2.7 \pm 0.3	3.2 \pm 1.3	6.3 \pm 2.8		
		Kingfisher	Brae Unit 1	8a-8	3886–3955	82.5 \pm 3.7	2.9 \pm 0.5	3.7 \pm 1.3	6.3 \pm 2.2	4.6 \pm 1.4
		Kingfisher	Brae Unit 2	8a-4	3990–4126	82.2 \pm 2.1	1.6 \pm 0.5	3.3 \pm 1.0	7.0 \pm 1.9	5.9 \pm 2.1

Table 2

SIMS results and interpretation of quartz phases (authigenic (AQ), detrital (DQ) or mix of both) and quartz cement CL zones (complex or homogeneous) which were analysed in oil and water zone samples from Brae Formation sandstones

Analysis number	Raw $^{18}\text{O}/^{16}\text{O}$ ($\times 1000$)	Corr. $^{18}\text{O}/^{16}\text{O}$ ($\times 1000$)	Standard error (‰)	$\delta^{18}\text{O}$ (‰) SMOW	Comment
<i>Miller-Brae Unit 2 reservoir-oil zone sample 3993.8</i>					
A13163A1	1.91397	1.888590611	1.4	25.8	AQ/homogeneous
A13163A2	1.89158	1.888296716	1.1	14.0	DQ
A13163A3	1.9117	1.88800282	1.3	24.9	AQ/homogeneous
D13163B1	1.8949	1.892705145	1.2	13.4	DQ
D13163B2	1.89482	1.89241125	1.3	13.5	DQ
A13163B3	1.90583	1.892117354	1.4	19.5	AQ/homogeneous
D13163B4	1.89314	1.891823459	1.0	12.9	detrital
A13163B5	1.90076	1.891529564	1.1	17.1	AQ/complex
A13163B6	1.90884	1.891235668	1.3	21.6	AQ/homogeneous
A13163B7	1.91259	1.890941773	1.2	23.8	AQ/homogeneous
A13163C1	1.90868	1.889472297	1.0	22.5	AQ/homogeneous
A13163C2	1.89555	1.889178401	1.0	15.6	AQ/complex
D13163C3	1.89838	1.888884506	45.5	17.3	mix
<i>Miller-Brae Unit 2 reservoir-oil zone sample 4039.6</i>					
A15312A1	1.88718	1.891309396	1.1	10.0	DQ
A15312A2	1.88935	1.890667423	1.2	15.5	AQ/complex
A15312A3	1.90226	1.891095405	1.4	18.2	AQ/complex
A15312A4	1.89267	1.890881414	1.1	16.2	AQ/complex
D15312B1	1.88247	1.888955494	1.4	8.7	DQ
A15312B2	1.8926	1.888741503	1.3	14.3	mix
A15312B3	1.89727	1.888527511	1.1	16.9	AQ/homogeneous
A15312B4	1.90216	1.88831352	1.2	19.6	AQ/homogeneous
A15312B5	1.89112	1.888099529	1.9	13.8	mix
A15312B6	1.90687	1.887885538	0.9	22.4	AQ/homogeneous
D15312C1	1.88418	1.89195137	1.2	8.1	DQ
A15312C2	1.87787	1.891737378	1.3	4.8	mix
A15312C3	1.88953	1.891523387	1.3	11.1	DQ
D15312D1	1.88825	1.89387729	1.4	9.2	DQ
A15312D2	1.89915	1.893663299	1.3	15.1	mix
A15312D3	1.88504	1.893449307	1.1	7.7	DQ
A15312D4	1.8978	1.893235316	1.3	14.7	mix
A15312D5	1.90726	1.893021325	1.2	19.8	AQ/homogeneous
A15312D6	1.8999	1.892807334	1.4	16.0	AQ/homogeneous
<i>Miller-Brae Unit 2 reservoir-water zone sample 4110.4</i>					
A5939A1	1.89637	1.891135631	1.1	15.0	DQ
A5939A2	1.90683	1.891056191	1.1	20.7	AQ/homogeneous
A5939A3	1.91152	1.890976752	1.2	23.2	AQ/homogeneous
A5939A4	1.90226	1.890897313	1.2	18.3	mix
A5939A5	1.89697	1.890817874	1.4	15.5	AQ/complex
A5939A6	1.9137	1.890738434	1.1	24.5	AQ/homogeneous
A5939B1	1.89745	1.890102921	1.1	16.1	AQ/complex
A5939B2	1.90978	1.890023481	1.3	22.8	AQ/homogeneous
A5939B3	1.89858	1.889944042	1.2	16.8	AQ/homogeneous
A5939B4	1.90658	1.889387967	1.1	21.4	AQ/homogeneous
A5939B5	1.89951	1.889308528	1.2	17.7	mix
A5939B6	1.89681	1.889229089	1.2	16.3	mix
A5939C1	1.90406	1.890658995	1.3	19.4	AQ/homogeneous
A5939C2	1.89614	1.890341238	1.0	15.3	mix

(continued on next page)

Table 2 (continued)

Analysis number	Raw $^{18}\text{O}/^{16}\text{O}$ ($\times 1000$)	Corr. $^{18}\text{O}/^{16}\text{O}$ ($\times 1000$)	Standard error (‰)	$\delta^{18}\text{O}$ (‰) SMOW	Comment
<i>Miller-Brae Unit 2 reservoir-water zone sample 4110.4</i>					
A5939C3	1.91249	1.890261799	1.1	24.1	AQ/homogeneous
A5939C4	1.90904	1.89018236	1.2	22.3	AQ/homogeneous
A5939D1	1.90246	1.889626285	1.3	19.1	AQ/homogeneous
A5939D2	1.89574	1.889546846	1.4	15.5	mix
A5939D3	1.90777	1.889467407	1.1	22.0	AQ/homogeneous
<i>Kingfisher-Brae Unit 1 reservoir-oil zone sample 3887.5</i>					
D13337A1	1.89868	1.888826917	1.0	17.5	DQ
A13337A2	1.89295	1.888859235	1.1	14.4	DQ
A13337A3	1.88232	1.888891553	1.0	8.7	DQ
A13337A5	1.8961	1.88892387	1.1	16.1	AQ/complex
A13337A6	1.91048	1.888956188	1.0	23.7	AQ/homogeneous
D13337C0	1.89659	1.887011904	1.2	17.3	DQ
D13337C1	1.89445	1.887227816	1.3	16.1	DQ
A13337C2	1.90976	1.887155846	1.0	24.3	AQ/homogeneous
A13337C3	1.90676	1.887083875	1.2	22.8	AQ/homogeneous
A13337C4	1.90134	1.886939933	1.1	19.9	mix
A13337C5	1.90811	1.886867963	1.2	23.6	AQ/homogeneous
A13337C6	1.90085	1.886795992	1.0	19.7	AQ/homogeneous
D13337C7	1.88602	1.888988506	1.1	10.6	DQ
D13337E1	1.89327	1.889117777	1.0	14.4	DQ
A13337E2	1.89799	1.889150095	1.0	16.9	AQ/complex
A13337E3	1.89488	1.889182413	0.9	15.3	AQ/complex
A13337E4	1.88833	1.88921473	1.2	11.7	DQ
A13337E5	1.89177	1.889247048	1.2	13.6	mix
A13337E6	1.89928	1.889311684	1.0	17.6	mix
A13337E7	1.90209	1.889279366	1.0	19.1	AQ/homogeneous
A13337E8	1.90741	1.889020824	1.0	22.1	AQ/homogeneous
<i>Kingfisher-Brae Unit 1 reservoir-oil zone sample 3904.2</i>					
D13395A1	1.88239	1.88852329	1.2	8.9	DQ
A13395A2	1.90347	1.888451319	1.2	20.3	AQ/homogeneous
A13395A3	1.88708	1.888379349	1.3	11.5	mix
A13395A4	1.88374	1.888307378	1.1	9.8	DQ
A13395A5	1.90143	1.888235407	1.3	19.3	AQ/homogeneous
A13395A6	1.90016	1.888163436	1.2	18.6	AQ/homogeneous
D13395B1	1.8834	1.887803583	1.0	9.8	DQ
A13395B2	1.90452	1.887731612	1.1	21.2	AQ/homogeneous
A13395B3	1.90994	1.887659641	1.3	24.2	AQ/homogeneous
A13395B4	1.89526	1.88758767	1.2	16.3	mix
A13395B5	1.89234	1.8875157	1.0	14.8	mix
A13395B6	1.89838	1.887443729	1.2	18.1	mix
A13395E1	1.88962	1.882854535	1.2	15.8	AQ/complex
A13395E2	1.87628	1.882748926	1.2	8.7	DQ
D13395F1	1.87384	1.883276972	1.1	7.1	DQ
A13395F2	1.87329	1.883171363	1.0	6.9	DQ
A13395F3	1.90041	1.883065753	1.1	21.5	AQ/homogeneous
A13395F4	1.89478	1.882960144	1.2	18.6	AQ/homogeneous
<i>Kingfisher-Brae Unit 1 reservoir-oil zone sample 3938.4</i>					
D13512A1	1.88141	1.885070638	1.1	10.2	DQ
A13512A3	1.8996	1.885137604	1.0	20.0	AQ/homogeneous
13512A3	1.90283	1.88520457	1.0	21.7	AQ/homogeneous

Table 2 (continued)

Analysis number	Raw $^{18}\text{O}/^{16}\text{O}$ ($\times 1000$)	Corr. $^{18}\text{O}/^{16}\text{O}$ ($\times 1000$)	Standard error (%)	$\delta^{18}\text{O}$ (‰) SMOW	Comment
<i>Kingfisher-Brae Unit 1 reservoir-oil zone sample 3938.4</i>					
13512B0	1.87913	1.885673333	1.0	8.7	DQ
13512B1	1.88969	1.885874232	1.1	14.3	mix
13512B2	1.90047	1.885941198	1.0	20.0	AQ/homogeneous
13512B3	1.90499	1.8857403	1.1	22.5	AQ/homogeneous
A13512B4	1.89023	1.886008164	1.0	14.5	mix
13512B5	1.89792	1.885807266	1.0	18.7	AQ/homogeneous
A13512B6	1.88735	1.88607513	1.1	12.9	DQ
D13512E1	1.8803	1.889440955	0.8	7.3	DQ
A13512E2	1.90823	1.889473272	1.0	22.3	AQ/homogeneous
A13512E3	1.90375	1.88950559	1.1	19.8	AQ/homogeneous
A13512E4	1.91081	1.889537908	1.0	23.6	AQ/homogeneous
A13512E6	1.90286	1.889570226	1.0	19.3	AQ/homogeneous
A13512E7	1.9122	1.889602543	1.0	24.3	AQ/homogeneous
A13512E8	1.90701	1.889634861	0.9	21.5	AQ/homogeneous
A13512F1	1.90117	1.885405469	0.9	20.7	AQ/homogeneous
A13512F2	1.90586	1.885338502	0.9	23.2	AQ/homogeneous
A13512F3	1.88765	1.885271536	1.0	13.5	mix
<i>Kingfisher-Brae Unit 2 reservoir-oil zone sample 3989.7</i>					
A13143A0	1.90048	1.877550829	1.1	24.6	AQ/homogeneous
D13143A1	1.87449	1.877594915	1.3	10.5	DQ
A13143A2	1.88972	1.877462655	1.2	18.8	mix
A13143A3	1.89478	1.877418569	1.3	21.6	AQ/homogeneous
A13143A4	1.89208	1.877374482	1.2	20.1	AQ/homogeneous
A13143A6	1.8793	1.877506742	1.1	13.2	mix
D13143C1	1.87932	1.878388475	1.1	12.7	DQ
A13143C2	1.8772	1.878344388	1.1	11.6	DQ
A13143C3	1.88842	1.878300301	0.9	17.7	AQ/homogeneous
A13143C4	1.89606	1.878256215	1.0	21.8	AQ/homogeneous
A13143C5	1.89142	1.878212128	0.9	19.3	mix
A13143D1	1.8872	1.878035782	1.1	17.1	AQ/homogeneous
A13143D2	1.90031	1.877991695	1.1	24.2	AQ/homogeneous
A13143D3	1.89453	1.877947608	1.1	21.2	AQ/homogeneous
A13143D4	1.90128	1.877903522	1.1	24.8	AQ/homogeneous
A13143D5	1.89473	1.877859435	1.0	21.3	AQ/homogeneous
A13143D6	1.8951	1.877815348	1.1	21.5	AQ/homogeneous
A13143D7	1.88595	1.877771262	1.1	16.6	mix
<i>Kingfisher-Brae Unit 2 reservoir-water zone sample 4030.3</i>					
A13274A1	1.89539	1.879730485	1.0	20.6	AQ/homogeneous
A13274B1	1.87733	1.879548792	1.0	11.0	DQ
A13274B2	1.9016	1.879609356	1.0	24.1	AQ/homogeneous
A13274B3	1.88947	1.87966992	1.0	17.5	AQ/homogeneous
A13274C1	1.8978	1.879427663	1.1	22.1	AQ/homogeneous
A13274C2	1.89658	1.879488227	1.1	21.4	mix
A13274D2	1.90198	1.880154436	1.1	24.0	AQ/homogeneous
D13274D3	1.87964	1.880215	1.1	11.9	DQ
A13274D4	1.8964	1.880093871	1.1	21.0	AQ/homogeneous
A13274D5	1.88199	1.880033307	1.0	13.3	mix
A13274D7	1.90117	1.879972742	1.1	23.6	AQ/homogeneous
A13274D9	1.88241	1.879912178	1.1	13.6	mix
D13274E1	1.88337	1.880699515	1.2	13.6	DQ

(continued on next page)

Table 2 (continued)

Analysis number	Raw $^{18}\text{O}/^{16}\text{O}$ ($\times 1000$)	Corr. $^{18}\text{O}/^{16}\text{O}$ ($\times 1000$)	Standard error (%)	$\delta^{18}\text{O}$ (‰) SMOW	Comment
<i>Kingfisher-Brae Unit 2 reservoir-water zone sample 4030.3</i>					
A13274E2	1.90121	1.880638951	1.0	23.3	AQ/homogeneous
A13274E3	1.89141	1.880578386	1.1	18.0	mix
A13274E4	1.89621	1.880517822	1.0	20.7	mix
A13274E5	1.89272	1.880457258	1.0	18.8	mix
A13274E6	1.89714	1.880396693	1.1	21.2	AQ/homogeneous
<i>Kingfisher-Brae Unit 2 reservoir-water zone sample 4081.0</i>					
D13437A1	1.87754	1.884966716	1.0	8.2	DQ
A13437A2	1.89695	1.884861107	1.1	18.7	AQ/homogeneous
A13437A3	1.90235	1.884755498	0.9	21.7	AQ/homogeneous
A13437A4	1.90080	1.884649889	0.9	20.9	AQ/homogeneous
A13437A5	1.89655	1.88454428	1.1	18.7	mix
A13437A5	1.90279	1.884438671	1.0	22.1	AQ/homogeneous
A13437A7	1.90094	1.884016235	0.9	21.3	mix
A13437A8	1.90178	1.883910626	1.0	21.8	AQ/homogeneous
A13437A9	1.88878	1.883805017	1.1	14.9	DQ
A437A10	1.90091	1.883699408	1.2	21.5	AQ/homogeneous
A437A11	1.89785	1.883593799	1.1	19.9	AQ/homogeneous
D437A14	1.8823	1.884121844	1.1	11.2	DQ

Miller and Kingfisher Fields (Giles et al., 2000; Marchand et al., 2000, 2002). The precipitation of quartz overgrowths in many sedimentary basins commonly occurs during deep burial diagenesis (>2.5 km) at elevated temperatures, typically 70–130 °C (e.g. Giles et al., 1992; Gluyas et al., 1993; Walderhaug, 1994; Bjørkum et al., 1998). Small amounts of quartz cement may, however, develop slowly at lower temperatures (<70 °C) given enough time (Bjørkum et al., 1998). There is evidence of some early quartz cementation in the Brae Formation sandstones. Small quantities (<1%) of quartz overgrowths have been observed in early diagenetic concretions (Marchand et al., 2000) (Fig. 2A). High minus-cement porosities (25–35%) determined in thin section samples of concretions, and oxygen isotope analyses of the calcite cement, indicate that calcite precipitated from meteoric water during shallow burial (<1.5 km) (Marchand et al., 2000). Reconstructed burial and temperature history models of the Brae Formation in the Miller and Kingfisher Fields indicate that at around 1.5 km burial, the sandstones were at approximately 60 °C (Fig. 3). The quartz overgrowths in the concretions petrographically predate the calcite cement and must therefore have grown at temperatures <60 °C. However, the lowest homogenization temperatures measured in fluid inclusions in quartz cements outside calcite-cemented zones are around 70

°C in all three reservoirs examined (Fig. 4). The lack of low-temperature (<70 °C) measurements in fluid inclusions can be explained by the fact that the earliest quartz cement occurs only in small quantities (<1%). Therefore, the likelihood of finding low-temperature inclusions is small. Also, fluid inclusions trapped close to earth surface conditions (<60 °C) generally occur as metastable all-liquid inclusions and may never nucleate a vapor bubble necessary for temperature measurement (Goldstein and Reynolds, 1992). The main phase of quartz cementation in the Brae Formation sandstones is interpreted to have occurred at deeper burial (>1.5 km). Fluid inclusion temperatures (Fig. 4) indicate quartz growth from 70 °C onwards up to present-day reservoir temperatures (120 °C; Rooksby, 1991). As explained in Marchand et al. (2002), the volume of quartz cement precipitated in each reservoir examined is directly linked to the time and duration of oil emplacement. Marchand et al. (2001) demonstrated that when oil displaced formation water from the pore-space in the Brae Formation sandstones, the quartz precipitation rate was reduced by at least two orders of magnitude. As a consequence, quartz cement abundances are lowest (<6%) in the crestal parts of the Brae Unit 2 reservoir in the Miller Field and in the entire Brae Unit 1 reservoir in the Kingfisher Field, which both filled with oil around 40 Ma (Marchand et al., 2002). Maximum fluid

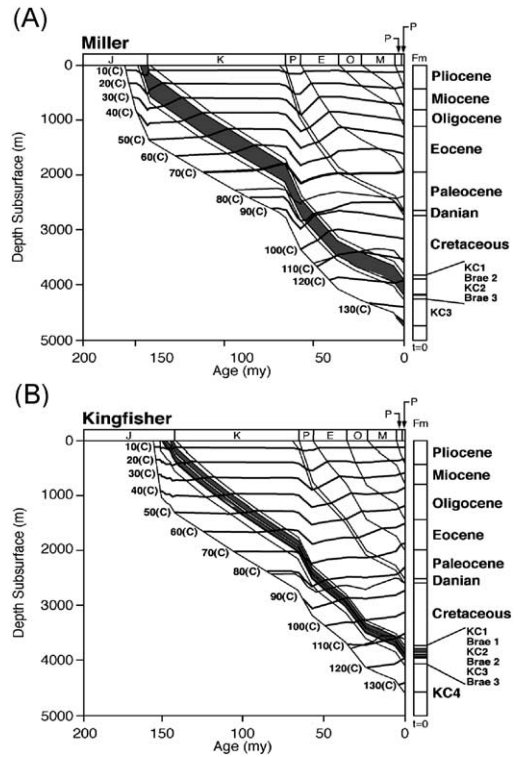
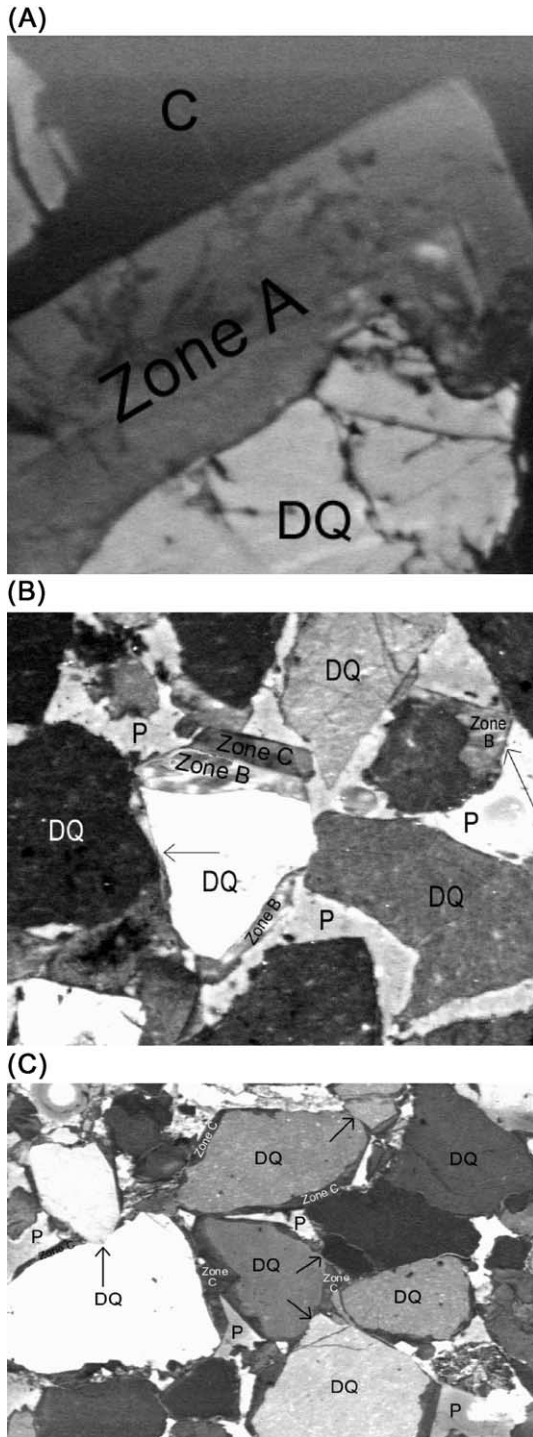


Fig. 3. Burial histories combined with isotherms for (A) Miller and (B) Kingfisher Field. The reservoir intervals studied are shaded grey (Brae Units 1 and 2) (after Marchand et al., 2002).

inclusion temperatures from oil zone samples in those reservoirs are up to 15 °C lower (i.e. 105 °C) than present-day bottom hole temperatures (120 °C; Rooksby, 1991), and are therefore in agreement with inhibition of quartz cementation due to displacement of pore water by hydrocarbons (Fig. 4). The Miller Field experienced gradual oil emplacement over a prolonged period of time (Marchand et al., 2001) and, as a consequence, quartz cement abundances

Fig. 2. SEM-CL images illustrating the different appearance of quartz cement zones in the Brae Formation sandstones. (A) Early diagenetic zone A quartz cement in calcite-cemented sandstone displays a homogeneous CL pattern (Miller Field sample, 3992.3 m, field of view 170 × 200 μm). (B) Zone B quartz cements display a complex CL pattern (Miller Field sample, 4022.7 m, field of view 625 × 500 μm). Arrows indicate cementation in pore space between detrital grains. (C) Zone C quartz cements display a homogeneous CL pattern (Kingfisher Field sample, 4023.6 m, field of view 1300 × 1000 μm). Arrows indicate detrital grains in point-contact with each other. C = calcite cement, DQ = detrital quartz and P = porosity.

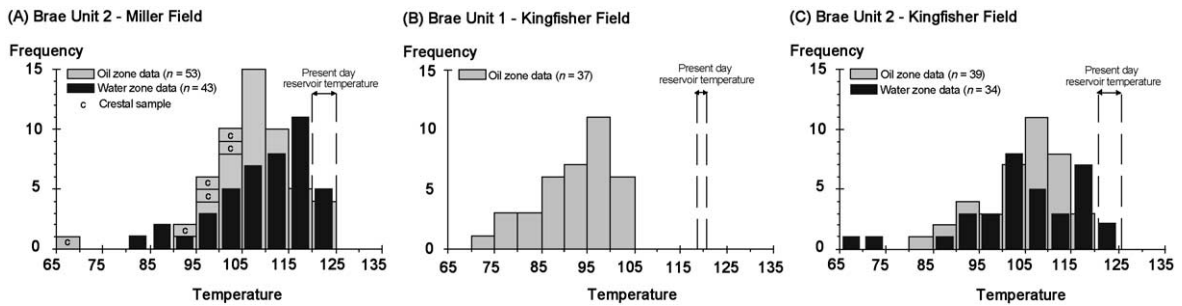


Fig. 4. Histograms of homogenization temperatures (T_h) measured in aqueous fluid inclusions in quartz cement. (A) T_h data from the Brae Unit 2 reservoir in the Miller Field suggest that quartz cementation was active around 65 °C and that oil zone cementation (peak histogram between 105 and 110 °C) is retarded compared to aquifer cementation (peak histogram between 115 and 120 °C). The highest temperatures measured in fluid inclusions in crestal samples (c) from the field are between 100 and 105 °C. (B) T_h data from the Brae Unit 1 reservoir in the Kingfisher Field suggest that quartz cementation was active around 70 °C and was halted when the reservoir was buried to temperatures of 95–105 °C (maximum measured temperatures). (C) T_h data from the Brae Unit 2 reservoir in the Kingfisher Field suggest that quartz cementation occurred over an analogous temperature range in oil and water zones of the reservoir (65–125 °C) (after Marchand et al., 2002).

and fluid inclusion temperatures increase (up to 10% and 120 °C; Marchand et al., 2001) in samples towards the oil–water contact at 4090 m (Fig. 4). The Brae Unit 2 reservoir in the Kingfisher Field contains significantly more quartz cement (8–12%). This reservoir filled with oil recently (around 10 Ma) and therefore quartz precipitated unhindered over a long period of time (Marchand et al., 2002). This is also reflected in fluid inclusion temperatures approaching present-day bottom hole temperatures (120 °C) in oil zone samples (Fig. 4). Quartz cement abundances are also high (10–15%; Marchand et al., 2002), and fluid inclusion temperatures extend up to 120 °C (Fig. 4) in the aquifers of the different reservoirs examined.

4.2. Quartz cement paragenesis

CL photomicrograph petrography of quartz overgrowths in the Brae Formation sandstones shows the presence of at least three cement zones (A, B and C) in all three reservoirs studied (Fig. 2). Zone A and zone C cements display a homogeneous CL pattern, whereas zone B quartz cements display a complex CL pattern (Fig. 2).

The earliest quartz cement zone to have precipitated must be zone A (homogeneous CL pattern) in the calcite concretions (i.e. <1.5 km and <60 °C) (Fig. 2A). The absence of zone B (complex CL pattern) in the early diagenetic concretions indicates that zone B quartz cements precipitated after calcite cementation occurred in the sandstones (i.e. >60 °C). Zone B is

rarely observed in the quartz cements, but where it does occur, it usually borders detrital grains (Fig. 2B). The thickness of this growth zone varies throughout the reservoirs and ranges between <5 to 30 µm. Zone B cements are often observed to fill pore space between detrital grains, indicating that cementation may have occurred before mechanical compaction was completed in the sandstones (Fig. 2B). Mechanical compaction in quartz-rich sandstones, such as the Brae Formation sandstones, stabilises when about 30% (Houseknecht, 1987) to 26% (Paxton et al., 1990) porosity is reached. This commonly corresponds to burial depths between 1.5 and 2.5 km. Between that depth range, when zone B cements were most likely precipitated, the Brae Formation sandstones were at temperatures between 60 and 90 °C (Fig. 3). Zone C (homogeneous CL pattern) quartz cement is the most common and makes up most of the bulk volume of the quartz cements in the Brae Formation. The zone C overgrowths can be up to 50 µm thick and precipitated mainly on grains which are partly in point-contact with each other, indicating a post-compactional, and post zone B cementation, origin (Fig. 2C). Therefore, zone C cementation most likely occurred at temperatures >90 °C (post-compaction).

4.3. Sources of silica for quartz cementation

The Brae Formation sandstones are quartzose or sublithic/arkosic arenites in composition in all three reservoirs studied (Table 1). Apart from localized

extensive calcite cemented volumes, authigenic minerals in the porous sands other than quartz are restricted to <2% bulk volume of kaolinite, dispersed minor calcite and pyrite (Marchand et al., 2002). Sources of silica inherent in the sandstones may be dissolution of K-feldspars, dissolution of biogenic silica (sponge spicules) and pressure dissolution of quartz at grain contacts or stylolites. Illitisation of kaolinite also releases silica to the pore waters in sandstones (Bjørlykke and Egeberg, 1993). However, the studied sandstones do not show any significant illitisation of the very small amounts of kaolinite present. Silica precipitated from meteoric water (e.g. Blatt, 1979; McBride, 1989) and silica released from interbedded shales during compaction (e.g. Sullivan and McBride, 1991; Gluyas et al., 2000) can also be considered as potential silica sources.

Petrographic observations and mass balance calculations indicate that only a small proportion (<2%) of the quartz cements in the Brae Formation reservoirs studied could have come from K-feldspar and sponge spicule dissolution (Marchand, 2001). This dissolution occurred most likely during shallow burial when the sandstones were open to meteoric water through-flow (Marchand et al., 2000). Because meteoric water is usually supersaturated with silica (Blatt, 1979), the silica released from K-feldspar and sponge spicule dissolution may have been sufficient to explain precipitation of the small amounts of zone A quartz cements (<1%) in the reservoirs during shallow burial (<1.5 km). The bulk of the quartz cements (zones B and C) in the Brae Formation sandstones were precipitated during deeper burial and at higher temperatures (>70 °C). Gluyas et al. (2000) calculated that clay mineral reactions in mudstones interbedded with the Brae Formation reservoir rocks can account for the volumes of

quartz cement observed. There is also abundant evidence in the sandstones, and in small laminae of interbedded argillaceous sandstones, of grain-to-grain pressure dissolution and stylolites (Fig. 5). Therefore, it is likely that also pressure solution contributed to the

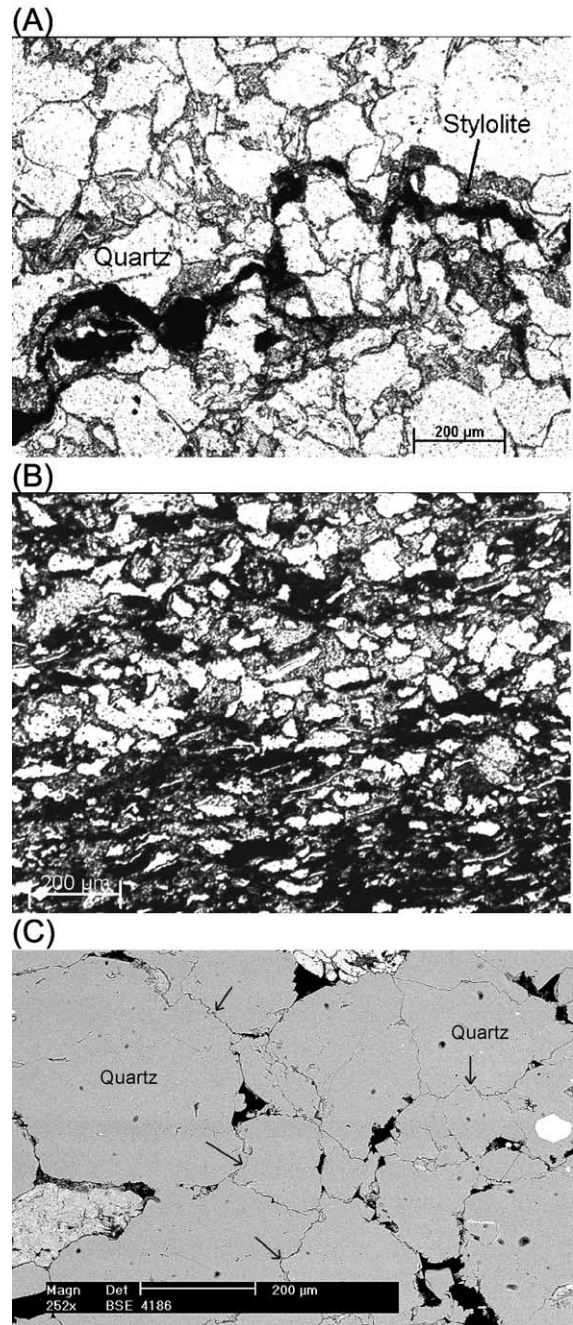


Fig. 5. (A) Plane-polarised light photomicrograph of stylolite seams in a sample of the Miller Field (4037 m). Quartz grains adjacent to the stylolite are irregular-shaped and smaller in size compared to quartz grains further away from the stylolite suggesting solution of detrital quartz at the stylolite interface. (B) Plane-polarised light photomicrograph of pressure solution of quartz grains embedded in argillaceous matrix in a sample of the Miller Field (4043 m). Silica dissolved in fine-grained laminae may diffuse to precipitation sites in nearby medium-grained sandstones and precipitate as quartz cement. (C) Backscatter SEM image of solution of detrital quartz at grain contacts between grains in a sample of the Kingfisher Field (4081 m). In some places, this process has produced sutured grain-contacts (arrows).

silica budget. On balance, both processes (pressure solution and clay mineral reactions) can account for the volume of quartz cements observed in the Brae Formation sandstones. The relative importance of each

process could not be judged because we did not quantitatively constrain pressure dissolution and/or silica released from clay mineral reactions in the samples studied.

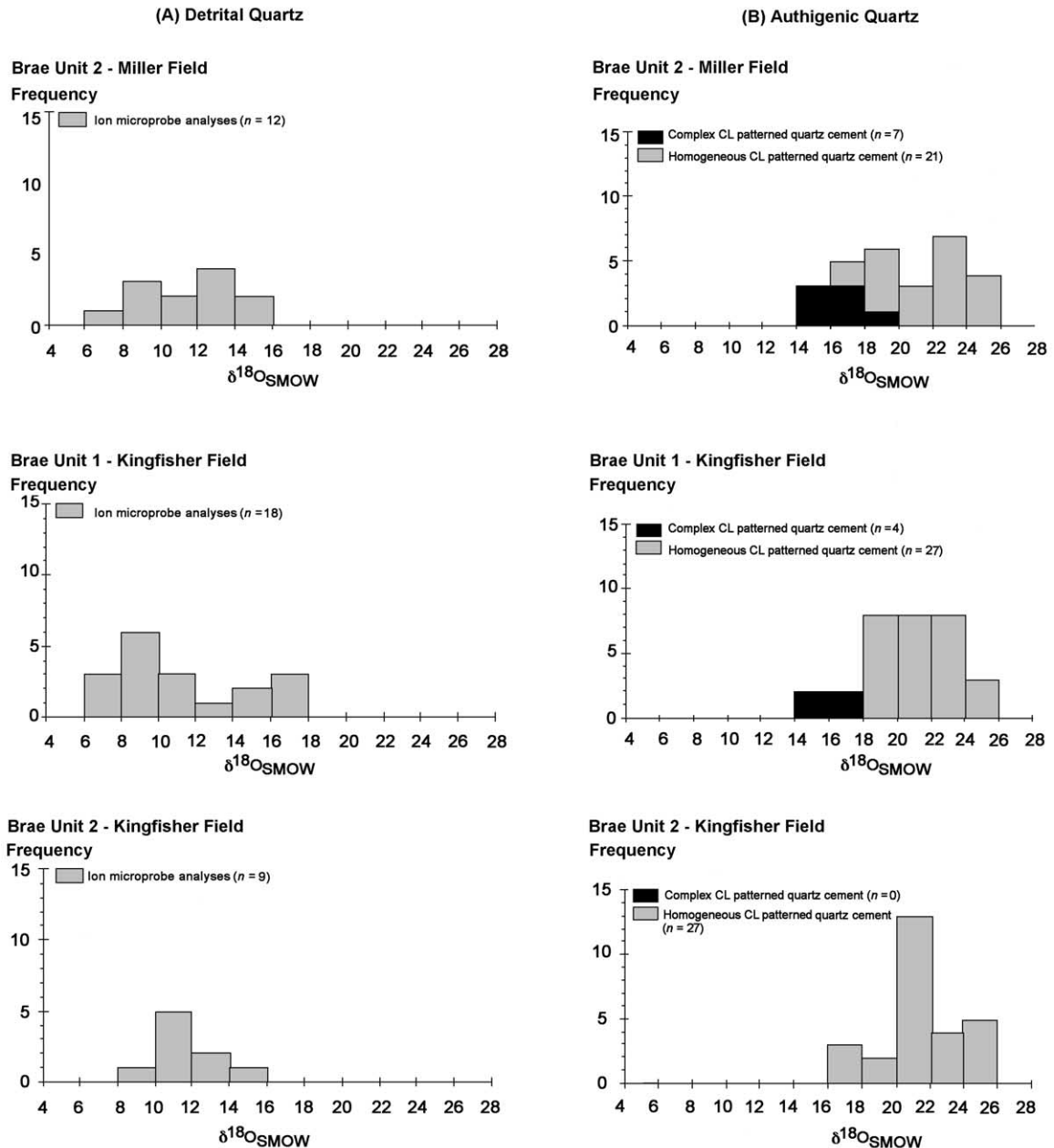


Fig. 6. Histograms showing the distribution of (A) detrital quartz and (B) authigenic quartz oxygen isotope values determined with the ion microprobe in the three reservoirs examined.

5. Oxygen isotope results

5.1. Data quality control

The oxygen isotope data obtained with the ion microprobe are listed in Table 2. Due to the small magnification in the optical microscope ($10\times$) on the ion microprobe, it is essential to check where the primary ion beam hit the sample before making any data interpretation. Bombardment with the primary ion beam results in a sputter pit on the polished sections. These sputter pits are typically 20–25 μm in diameter. The location of the sputter pits made by analyses in each thin section was checked by SEM (in SE and CL operating mode). In Table 2, an interpretation of the location of the sputter pits (in authigenic quartz, detrital quartz or overlapping both) is inserted in the ‘comment’ column. The mixed signatures were not used for interpretation.

5.2. Detrital quartz

The histograms shown in Fig. 6A summarize the $\delta^{18}\text{O}$ range of the 39 microanalyses of detrital quartz carried out with the ion microprobe. Both authigenic and detrital quartz can show cathodoluminescence (CL) at various intensities, but there is usually a marked contrast between them in individual grains, as illustrated by our CL photomicrographs (Fig. 2). The $\delta^{18}\text{O}$ of detrital quartz grains in the Brae Formation sandstone reservoirs examined ranges from

+6.9‰ to +17.5‰ (average 11.4 ± 2.8 ‰). The significant intragrain variations in detrital quartz $\delta^{18}\text{O}$ are of comparable magnitude to heterogeneities measured in quartz from granitic rocks (Valley and Graham, 1996). According to Blatt (1987), average $\delta^{18}\text{O}$ of quartz in igneous rocks is around +9‰, in metamorphic rocks around +13 to +14‰ and in sandstones around +11‰. The average of all analyses in detrital quartz grains of the Brae Formation sandstones is similar in all three reservoirs examined: 11.4 ± 2.6 ‰ in Brae Unit 2 of the Miller Field, 11.2 ± 3.5 ‰ in Brae Unit 1 of the Kingfisher Field and 11.7 ± 1.9 ‰ in Brae Unit 2 of the Kingfisher Field. These numbers are similar to Blatt’s data for the detrital component of sandstones (~ 11 ‰). The wide range in oxygen isotopic compositions of the detrital quartz grains analysed (+6.9 to +17.5‰) is consistent with granitic and/or metamorphic terranes being the predominant source of the detrital quartz in the Brae Formation sandstones. A similar range and average of $\delta^{18}\text{O}$ values in each reservoir examined suggests a similar source region for quartz across the whole Brae Formation. The most likely source region, as suggested by McClure and Brown (1990), is the Devonian Fladen Ground Spur (Fig. 1).

5.3. Authigenic quartz

The histograms shown in Fig. 6B summarize the $\delta^{18}\text{O}$ values of the 86 microanalyses in authigenic

Table 3

Average (\pm standard deviation) $\delta^{18}\text{O}$ values of homogeneous and complex CL-patterned quartz cements in oil and water zone samples from Brae Formation sandstones

			CL zone	Average $\delta^{18}\text{O}_{\text{SMOW}}$ (‰)	Standard deviation (‰)	No. analyses	Range (‰)
Miller Field	Brae Unit 2 reservoir	oil zone	complex	16.5	1.1	5	15.5–18.2
			homogeneous	21.2	3.1	11	16.0–25.8
	water zone	complex	15.8	0.4	2	15.5–16.1	
		homogeneous	21.5	2.3	11	16.8–24.5	
Kingfisher Field	Brae Unit 1 reservoir	oil zone	complex	16	0.7	4	15.3–16.9
			homogeneous	21.4	1.9	27	18.6–24.3
	water zone	the sampled well did not contain an aquifer					
Kingfisher Field	Brae Unit 2 reservoir	oil zone	complex	–	–	–	–
			homogeneous	21.4	2.5	11	17.1–24.8
		water zone	complex	–	–	–	–
		homogeneous	21.5	1.8	16	17.5–24.1	

quartz. The $\delta^{18}\text{O}$ of authigenic quartz in the Brae Formation sandstone reservoirs examined ranges from +15.3‰ to +25.8‰ (average 20.8 ± 2.7 ‰). There is a wide spread in $\delta^{18}\text{O}$ values in all three reservoirs studied (Fig. 6B). The average oxygen isotopic composition of quartz cements is similar in each reservoir: 20.3 ± 3.2 ‰ in the Brae Unit 2 reservoir in the Miller Field, 20.7 ± 2.6 ‰ in the Brae Unit 1 reservoir in the Kingfisher Field and 21.5 ± 2.1 ‰ in the Brae Unit 2 reservoir in the Kingfisher Field.

Because it is not possible to petrographically differentiate the two generations of homogeneous luminescent quartz cements (zones A and C) in non-calcite-cemented samples, it was not possible to isotopically distinguish zones A and C cements in the ion microprobe analysis results (Table 2). Consequently, the oxygen isotope results below are discussed in terms of the two CL patterns occurring in quartz cement (homogeneous and complex). The two different quartz cement CL patterns are distinct in their oxygen isotopic compositions (Table 3 and Fig. 6). The $\delta^{18}\text{O}$ values measured in complex CL-patterned quartz cements (zone B cement only) range from +15.3‰ to +18.2‰ (Fig. 6). The average oxygen isotope signature is similar in oil and water zone samples of the two reservoirs where hydrocarbon emplacement occurred around 40 Ma, i.e. the Brae Unit 2 reservoir of the Miller Field and the Brae Unit 1 reservoir of the Kingfisher Field (Table 3). In the reservoir where oil charged recently (around 10 Ma), i.e. the Brae Unit 2 reservoir of the Kingfisher Field, no complex CL-patterned quartz cement was encountered for analysis (Fig. 6). In homogeneous CL-patterned quartz cements (zones A and C), $\delta^{18}\text{O}$ ranges between +16.0‰ and +25.8‰ (Table 3). The average oxygen isotopic signature of homogeneous CL-patterned quartz cements (zones A and C) is also similar in oil and water zone samples in all three reservoirs (Table 3).

6. Discussion

6.1. Petrographic constraints on pore water evolution

Pore water compositions in any basin change with time and increasing burial. In view of the wide range in measured quartz cement $\delta^{18}\text{O}$ values (+15.3 to

+25.8‰), reconstruction of the fluid evolution from the time of the earliest precipitation of quartz cements in the Brae Formation sandstones (at <1.5 km burial and <60 °C) until the present (4.0 km burial and 120 °C) is subject to considerable uncertainty, particularly since zone A (<1% of the quartz cement) may not be represented in the ion microprobe data. In order to calculate the $\delta^{18}\text{O}$ pore water compositions from the measured oxygen isotope signatures, the following information on quartz cement paragenesis needs to be taken into account:

- 1) the earliest quartz cement zone, A (homogeneous CL pattern), precipitated in the sandstones at temperatures <60 °C;
- 2) the second quartz cement zone, B (complex CL pattern), precipitated in the sandstones most likely between 70 and 90 °C;
- 3) the third quartz cement zone, C (homogeneous CL pattern), precipitated in the sandstones most likely at temperatures >90 °C.

Because there are no distinct fluid inclusion temperature peaks (Fig. 4) which could potentially distinguish the different zones of quartz cement, it is thought that cementation in the Brae Formation sandstones was more or less a continuous process; the changes in isotopic ratio in the cements may therefore be continuous also. The range in measured $\delta^{18}\text{O}$ values in quartz cements, and the occurrence of quartz cement zones, is similar in all three reservoirs examined. Consequently, it is reasonable to assume that pore water evolution was similar across the entire Brae Formation. The nature of pore waters in which silica for quartz cementation in the Brae Formation was transported is discussed below by means of oxygen isotope fractionation curves based upon the fractionation equation of Matsuhisa et al. (1979) (Fig. 7).

6.2. Geochemical constraints on pore water evolution

Oxygen isotope analyses of early calcite cements in the Brae Formation indicate that meteoric water was present in the sandstones at shallow burial depths (<1.5 km) (Marchand et al., 2000). Upper Jurassic meteoric water had an oxygen isotope composition estimated as ~ -7 ‰ (Hamilton et al., 1987). The

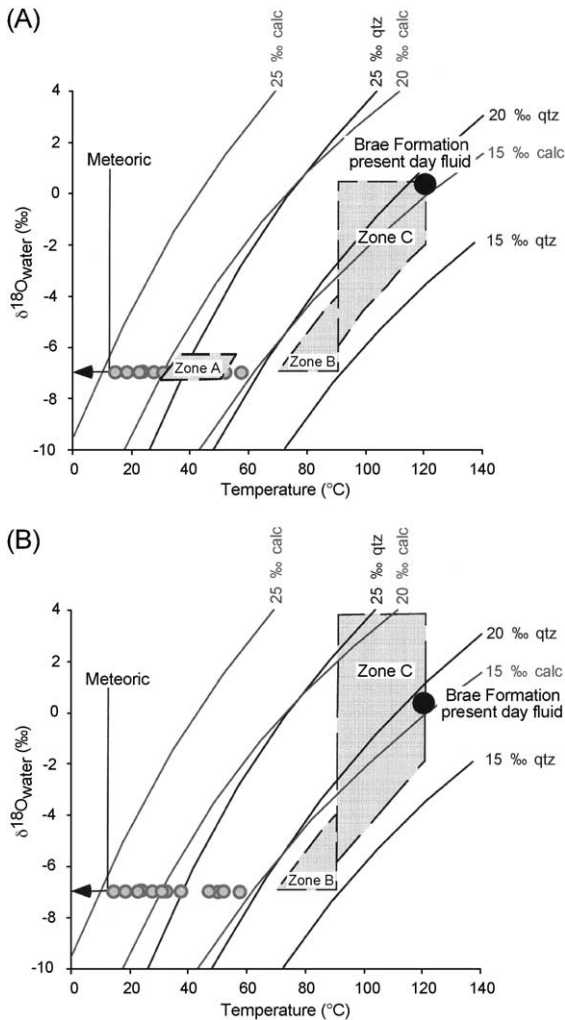


Fig. 7. Cross plots of pore water $\delta^{18}\text{O}$ values versus temperature showing oxygen isotope fractionation curves for calcite cement from +15‰ to +25‰ (grey; Friedman and O'Neil, 1977) and for quartz cement from +15‰ to +25‰ (black; Matsuhisa et al., 1979). Shaded areas outline measured quartz cement $\delta^{18}\text{O}$ compositions and grey circles represent measured calcite cement $\delta^{18}\text{O}$ compositions from Marchand et al. (2000). Two pore water evolution models (A) and (B) can be developed in order to explain quartz cement $\delta^{18}\text{O}$ compositions between +23‰ and +26‰. The pore water evolution model pictured in (A) is favoured for reasons outlined in the text.

measured $\delta^{18}\text{O}$ values in calcite cements are plotted onto Fig. 7. Present-day formation water isotopic composition in the Brae Formation is around +0.6‰ (Smalley and Warren, 1994) at 4.0-km burial

and temperatures around 120 $^{\circ}\text{C}$. Considering that the Brae Formation sandstones have been continuously buried since their time of deposition until the present (Fig. 3), oxygen isotope compositions of the pore waters from which quartz cements precipitated most probably range between Upper Jurassic meteoric water (-7‰) and present-day formation water (+0.6‰).

6.3. Pore water evolution

All zone B quartz cements (complex CL pattern), with $\delta^{18}\text{O}$ compositions between +15.5‰ and +18.2‰, most likely precipitated between 70 and 90 $^{\circ}\text{C}$. Pore water oxygen isotope compositions from which these zone B cements precipitated therefore correspond to meteoric-type fluids (~ -7 ‰) with a shift towards more ^{18}O -enriched fluids (~ -4 ‰) as temperatures approach 90 $^{\circ}\text{C}$ (Fig. 7). This shift in pore water isotopic composition during burial from 1.5 to 3.0 km is best explained by mixing of the meteoric-type fluids (-7‰) with basinal-type fluids (+2–+5‰; Egeberg and Aagaard, 1989, Wilkinson et al., 1992). Plausible evidence for the introduction of basinal-type fluids in the reservoirs may be (1) the high salinity (15–25 wt.% NaCl eq) of low-temperature (70–90 $^{\circ}\text{C}$) fluid inclusions (Marchand, 2001) which may indicate incorporation of dissolved salts from formations deeper in the basin (probably Zechstein) and (2) the coincidence of the arrival of basinal fluids in the reservoirs with the early stages of hydrocarbon emplacement (~ 40 Ma; Marchand et al., 2002) in the Brae Unit 2 reservoir of the Miller Field and the Brae Unit 1 reservoir of the Kingfisher Field. Considering hydrocarbons originate deeper in the basin than the reservoir's burial depth, the oil migration will most likely be accompanied by fluids of an isotopically more positive nature. The fact that no zone B cements were encountered for analysis in the Brae Unit 2 reservoir of the Kingfisher Field conforms with the recent oil charge (~ 10 Ma; Marchand et al., 2002) and may consequently not be just a mere coincidence.

Homogeneous CL-patterned quartz cements, with $\delta^{18}\text{O}$ compositions between +16.0‰ and +25.8‰, could be zone A or zone C cements. As mentioned earlier, only small amounts of zone A cement (<1%) developed in the early diagenetic calcite concretions at

temperatures < 60 °C. Therefore, the bulk of the homogeneous CL-patterned quartz cements analysed are most likely from the zone C generation which precipitated from ~ 90 °C onwards up to present-day reservoir temperatures (120 °C). The most plausible fluid evolution in the reservoir, which can explain most of the measured homogeneous CL-patterned quartz cement $\delta^{18}\text{O}$ compositions (i.e. $+16$ – $+22$ ‰), is that with increasing burial depth and temperature, quartz cements progressively precipitated from fluids which evolved in composition from a fluid with $\delta^{18}\text{O} \sim -4$ ‰ initially (~ 90 °C) to an end-member basinal-type fluid with $\delta^{18}\text{O}$ similar to the present-day formation water oxygen isotope composition ($+0.6$ ‰) (Fig. 7A). The continuous enrichment of pore water in ^{18}O may be attributed to ongoing oil charge and/or rock–water interactions in mudstones enclosing the sandstones. Possible reactions include illitisation and/or chloritisation of kaolinite and smectite clays formed by low-temperature weathering (Wilkinson et al., 1992) and/or recrystallisation of early formed carbonates (Saigal and Bjørlykke, 1987).

The measured $\delta^{18}\text{O}$ compositions between $+23$ ‰ and $+26$ ‰ in homogeneous CL-patterned quartz cements (zone A or zone C) are more difficult to explain. Two pore water evolution models can be developed to accommodate $\delta^{18}\text{O}$ values of $+23$ – $+26$ ‰ (Fig. 7):

- 1) if these homogeneous CL-patterned quartz cements correspond to zone A cements, then precipitation occurred from a meteoric-type fluid (most likely -7 ‰ to -6 ‰) at temperatures around 30 – 50 °C (Fig. 7A);
- 2) if these homogeneous CL-patterned quartz cements correspond to zone C cements, then precipitation occurred from a basinal-type fluid (most likely $+2$ ‰ to $+5$ ‰) at temperatures between 90 and 120 °C (Fig. 7B).

Although no low temperatures (< 50 °C) have been measured in fluid inclusions in quartz cements, the first model (Fig. 7A) is plausible for the following reasons: (1) there is evidence of early quartz cementation in the calcite-cemented sandstones (Fig. 2A) which suggests precipitation at shallow burial depths (< 1.5 km) and low temperatures (< 60 °C); (2) the

pore water composition derived for homogeneous CL-patterned quartz cements in this model (from -7 ‰ to -6 ‰) is in agreement with measured calcite cement $\delta^{18}\text{O}$ compositions across the 30 – 50 °C temperature range (Fig. 7A). Considering the marine depositional environment of the sandstones, the presence of waters with oxygen isotopic composition similar to meteoric water in the Brae Formation implies that the sandstones were open to surface water recharge during shallow burial (< 1.5 km). The high initial porosities (~ 35 – 40 %), and also permeabilities, in the sandstones during shallow burial were likely to have permitted meteoric water flow during the early stages of diagenesis when the adjacent graben margin was being uplifted and sub-aerially eroded. The model presented in Fig. 7B implies that the pore water $\delta^{18}\text{O}$ values decrease again to the present-day formation water composition ($+0.6$ ‰) after the influx of basinal fluids occurred. Therefore, although an increase of pore water $\delta^{18}\text{O}$ up to $+2$ – $+5$ ‰ due to the effect of ongoing hydrocarbon emplacement is attractive (however, $\delta^{18}\text{O}$ values up to 24.8 ‰ are also recorded in quartz cements in the Brae Unit 2 reservoir of the Kingfisher Field where oil-fill was recent; Table 2), a subsequent decrease to the present-day 0.6 ‰ is difficult to explain. Consequently, the pore water model in Fig. 7A where pore waters evolve continuously from meteoric-type fluids to the present-day formation water oxygen isotope composition seems more likely.

6.4. Comparison with pore water evolution in nearby areas

The Brent Group reservoirs are located approximately 150 km from the Brae Formation area in the northern North Sea. An integrated study of petrographic, fluid inclusion and oxygen isotope data from diagenetic minerals in Brent Group reservoirs, published by Haszeldine et al. (1992), reveals a pore water evolution similar to our Fig. 7A. According to Haszeldine et al. (1992), diagenesis in the first 2.0 km of burial (up to 70 °C) of Brent reservoirs occurred in the presence of meteoric water. As burial continued to present-day depth of the samples analysed by Haszeldine et al. (1992), i.e. up to 3.8 km, pore water oxygen isotopic composition evolved gradually from mete-

oric water (-7‰) to present-day formation water ($+2\text{‰}$) composition.

The Haltenbanken area on the Atlantic margin offshore Norway is located approximately 650 km from the Brae Formation area. Williams et al. (1997) identified three quartz cement phases which correspond with three palaeofluid phases in this area:

- 1) Phase I quartz with $\delta^{18}\text{O}$ values between $+23\text{‰}$ and $+26\text{‰}$ is interpreted to have precipitated from waters with $\delta^{18}\text{O}$ near -7‰ around 50 °C ;
- 2) Phase II quartz with $\delta^{18}\text{O}$ values between $+14\text{‰}$ and $+19\text{‰}$ is interpreted to have precipitated from waters with $\delta^{18}\text{O}$ between -5‰ and 0‰ as temperatures increase (up to 120 °C);
- 3) Phase III quartz with $\delta^{18}\text{O}$ values between $+20\text{‰}$ and $+23\text{‰}$ is interpreted to have precipitated from waters with positive $\delta^{18}\text{O}$ around present-day temperatures (140 °C).

The growth sequence of quartz cementation zones and measured $\delta^{18}\text{O}$ values, and the fluid evolution model derived from those results, in the Haltenbanken area mirrors the results and fluid evolution model for the Brae Formation area in the South Viking graben described in this paper. The fact that Williams et al. (1997) observed three quartz cementation zones with distinctive oxygen isotopic signatures also substantiates the validity of our definition of zone A cement in the Brae Formation sandstones and our preference for the pore water evolution model pictured in Fig. 7A. The quartz cement zone A in this study was derived from petrographic and textural relationships and is believed to correspond to the measured $\delta^{18}\text{O}$ values between $+23\text{‰}$ and $+26\text{‰}$. This cement zone corresponds with Williams et al.'s phase I quartz.

The similarity in pore water evolution across three distinct subbasins in the North Sea indicates that pore water evolution may occur through similar subsurface processes in many other areas. Considering quartz cement is a major porosity-occluding phase in many deeply buried sandstone reservoirs, and because pore waters both dissolve quartz and carry the dissolved silica to cementation sites, the data presented are a valuable contribution to constraints on reservoir quality predictions of exploration targets worldwide.

7. Conclusions

(1) The ion microprobe has facilitated in situ oxygen isotope analysis of quartz cements in polished thin sections with a spatial resolution of $\sim 20\text{ }\mu\text{m}$ and a precision on individual analyses of $\pm 1\text{‰}$.

(2) Based on petrographic, textural, fluid inclusion and basin modelling results, three phases of quartz cement, which precipitated progressively and sequentially as temperatures increased during burial, can be distinguished: (1) small amounts of zone A (homogeneous CL pattern) precipitated at temperatures $<60\text{ °C}$ and $<1.5\text{ km}$ burial; (2) zone B (complex CL pattern) precipitated most likely between 70 and 90 °C and from 1.5 to 3.0 km burial; (3) the bulk of the quartz cement, zone C (homogeneous CL pattern), precipitated most likely at temperatures $>90\text{ °C}$ and 3.0 km burial, up to present-day reservoir conditions (120 °C and 4.0 km).

(3) A wide range of detrital and authigenic quartz $\delta^{18}\text{O}$ compositions was obtained with the ion microprobe analysis technique. The oxygen isotopic compositions of detrital quartz grains in the Brae Formation sandstones range between $+6.9\text{‰}$ and $+17.5\text{‰}$. The wide range in detrital quartz $\delta^{18}\text{O}$ values indicates that the grains in the sandstones are a mixture of quartz from different origins (e.g. igneous quartz, metamorphic quartz). The oxygen isotopic compositions of authigenic quartz range between $+15.3\text{‰}$ and $+25.8\text{‰}$. The wide range in authigenic quartz $\delta^{18}\text{O}$ values indicates that quartz cements precipitated from different pore waters over a range of temperatures.

(4) Based on quartz cement petrography, the relationship to isotopically depleted shallow burial calcite cement, fluid inclusion precipitation temperatures and measured $\delta^{18}\text{O}$ compositions, three fluid-temperature regimes can be recognised in the Brae Formation sandstones. The most likely scenario is that zone A quartz cements (estimated $\delta^{18}\text{O}$ between $+23\text{‰}$ and $+26\text{‰}$) precipitated first from a meteoric-type fluid ($\sim -7\text{‰}$) during shallow burial ($<60\text{ °C}$ and $<1.5\text{ km}$). Subsequently, precipitation of zone B quartz cements ($\delta^{18}\text{O}$ between $+14\text{‰}$ and $+19\text{‰}$) during burial from ~ 1.5 to $\sim 3.0\text{ km}$ ($60\text{--}90\text{ °C}$) occurred from fluids with oxygen isotope signatures between -7‰ and -4‰ . The bulk of the quartz overgrowths, zone C, precipitated during burial from 3.0

km (90 °C) to present-day reservoir depths (4.0 km and 120 °C) from pore waters which evolved in oxygen isotope composition from $\sim -4\text{‰}$ to present-day formation water oxygen isotope composition ($+0.6\text{‰}$).

(5) The high initial porosities ($\sim 35\text{--}40\%$), and also permeabilities, in the sandstones during shallow burial are likely to have permitted silica transport by meteoric water flow during the early stages of diagenesis (<1.5 km and <60 °C). At deeper burial, the effect of increasing rock–water ratio and hydrocarbon emplacement resulted in progressive enrichment of the pore waters in ^{18}O until eventually the present-day formation water $\delta^{18}\text{O}$ composition ($+0.6\text{‰}$) was reached.

(6) Because the hydrocarbon charging history of any reservoir is a complex matter, and because we measured a wide range of $\delta^{18}\text{O}$ values, establishing a link between the oxygen isotope values measured in quartz cements and the hydrocarbon emplacement in the Brae Formation reservoirs is difficult. Our results do not prove that a relationship exists but can be interpreted to indicate a connection between the two processes. The deduced increase in pore water $\delta^{18}\text{O}$ values with time and burial indicates an influx of basinal-type waters which coincides with the early stages of oil-fill in the reservoirs.

(7) The fluid evolution models derived for Brent Group reservoirs in the northern North Sea (Haszeldine et al., 1992) and for the Haltenbanken area on the Atlantic margin (Williams et al., 1997) are very similar to the fluid evolution model for the Brae area of the South Viking graben described in this paper. The potential to compare high-resolution diagenetic patterns globally with a high degree of analytical certainty demonstrates the value of the SIMS analysis technique.

Acknowledgements

We thank especially John Craven for support during ion microprobe analytical sessions and for statistical data processing of SIMS data. Thin sections for this study were made by Mike Hall. We acknowledge BP and Shell UK for providing Miller and Kingfisher Field samples and Platte River

Associates (Denver) for providing BasinMod. The Edinburgh ion microprobe laboratory is supported by NERC. This study was partly funded by NERC grants GR3/R9702 and GST/02/2100. The authors thank Norman Oxtoby and Lynda Williams for their constructive comments which helped improve the manuscript. [EO]

References

- Bjørkum, P.A., Oelkers, E.H., Nadeau, P.H., Walderhaug, O., Murphy, W.M., 1998. Porosity prediction in quartzose sandstones as a function of time, temperature, depth, stylolite frequency, and hydrocarbon saturation. *AAPG Bull.* 82, 637–648.
- Bjørlykke, K., Egeberg, P.K., 1993. Quartz cementation in sedimentary basins. *AAPG Bull.* 77, 1538–1548.
- Bjørlykke, K., Aagaard, P., Dypvik, H., Hastings, D.S., Harper, A.S., 1986. Diagenesis and reservoir properties of Jurassic sandstones from the Haltenbanken area, offshore mid-Norway. In: Spencer, A.M., Holter, E., Campell, C.J., Hanslien, S.H., Nelson, P.H.H., Nysaether, E., Ormaasen, E.G. (Eds.), *Habitat of Hydrocarbons on the Norwegian Continental Shelf*. Graham and Trotman, London, pp. 275–286.
- Blatt, H., 1979. Diagenetic processes in sandstones. *Soc. Econ. Paleontol. Mineral. Spec. Publ.* 26, 141–157.
- Blatt, H., 1987. Oxygen isotopes and the origin of quartz. *J. Sediment. Petrol.* 57, 373–377.
- Brint, J.F., Hamilton, P.J., Haszeldine, R.S., Fallick, A.E., Brown, S., 1991. Oxygen isotopic analysis of diagenetic quartz overgrowths from the Brent sands: a comparison of two preparation methods. *J. Sediment. Petrol.* 61, 527–533.
- Egeberg, P.K., Aagaard, P., 1989. Origin and evolution of formation waters from oil fields on the Norwegian shelf. *Appl. Geochem.* 4, 131–142.
- Ehrenberg, S.N., 1990. Relationship between diagenesis and reservoir quality in sandstones of the Garn Formation, Haltenbanken, mid-Norwegian continental shelf. *AAPG Bull.* 74, 1538–1558.
- Elsenheimer, D., Valley, J.W., 1993. Submillimeter zonation of $\delta^{18}\text{O}$ in quartz and feldspar, Isle of Skye, Scotland. *Geochim. Cosmochim. Acta* 57, 3669–3676.
- Friedman, I., O'Neil, J.R., 1977. Compilation of stable isotope fractionation factors of geochemical interest. In: Fleischer, M. (Ed.), *U. S. Geol. Surv. Prof. Pap.*, vol. 440-kk, p. 12.
- Giles, M.R., Stevenson, S., Martin, S.V., Cannon, S.J.C., Hamilton, P.J., Marshall, J.D., Samways, G.M., 1992. The reservoir properties and diagenesis of the Brent Group: a regional perspective. In: Morton, A.C., Haszeldine, R.S., Giles, M.R., Brown, S. (Eds.), *Geology of the Brent Group*. Spec. Publ.-Geol. Soc. London, vol. 61, pp. 289–327.
- Giles, M.R., Indrelid, S.L., Beynon, G.V., Amthor, J., 2000. The origin of large-scale quartz cementation: evidence from large data sets and coupled heat-fluid mass transport modelling. In: Worden, R.H., Morad, S. (Eds.), *Quartz Cementation in Sandstones*. *Int. Assoc. Sedimentol., Spec. Publ.*, vol. 29, pp. 21–38.

- Gluyas, J.G., Robinson, A.G., Emery, D., Grant, S.M., Oxtoby, N.H., 1993. The link between petroleum emplacement and sandstone cementation. In: Parker, J.R. (Ed.), *Petroleum Geology of NW-Europe*. Geological Society, London, pp. 1395–1402.
- Gluyas, J., Garland, C., Oxtoby, N.H., Hogg, A.J.C., 2000. Quartz cement: the Miller's tale. In: Worden, R.H., Morad, S. (Eds.), *Quartz Cementation in Sandstones*. Int. Assoc. Sedimentol., Spec. Publ., vol. 29, pp. 199–218.
- Goldstein, R.H., Reynolds, T.J., 1992. Systematics of fluid inclusions in diagenetic minerals—notes for a short course. Short Course on Fluid Inclusions in Sedimentary Rocks, Newcastle Research Group, August 17–20, pp. 64.
- Graham, C.M., Valley, J.W., Winter, B.L., 1996. Ion microprobe analysis of $^{18}\text{O}/^{16}\text{O}$ in authigenic and detrital quartz in the St. Peter Sandstone, Michigan Basin and Wisconsin Arch, USA: contrasting diagenetic histories. *Geochim. Cosmochim. Acta* 60, 5101–5116.
- Hamilton, P.J., Fallick, A.E., Macintyre, R.M., Elliott, S., 1987. Isotopic tracing of the provenance and diagenesis of lower Brent Group Sands, North Sea. In: Brooks, J., Glennie, K. (Eds.), *Petroleum Geology of Northwest Europe*. Graham & Trotman, London, pp. 939–949.
- Hanor, J.S., 1980. Dissolved methane in sedimentary brines: potential effect on the PVT properties of fluid inclusions. *Econ. Geol.* 75, 603–609.
- Harms, J.C., Tackenberg, P., Pickles, E., Pollock, R.E., 1981. The Brae oilfield area. In: Illing, L.V., Hobson, G.D. (Eds.), *Petroleum Geology of the Continental Shelf of North-West Europe*. Heyden, London, pp. 352–357.
- Haszeldine, R.S., Brint, J.F., Fallick, A.E., Hamilton, P.J., Brown, S., 1992. Open and restricted hydrologies in Brent Group diagenesis: North Sea. In: Morton, A.C., Haszeldine, R.S., Giles, M.R., Brown, S. (Eds.), *Geology of the Brent Group*. Spec. Publ.-Geol. Soc. London, vol. 61, pp. 401–419.
- Houseknecht, D.W., 1987. Assessing the relative importance of compaction processes and cementation to reduction of porosity in sandstones. *AAPG Bull.* 71, 633–642.
- Land, L.S., Fisher, R.S., 1987. Wilcox sandstone diagenesis, Texas Gulf coast: a regional isotopic comparison with the Frio Formation. In: Marshall, J.D. (Ed.), *Diagenesis of Sedimentary Sequences*. Spec. Publ.-Geol. Soc. London, vol. 36, pp. 219–235.
- Lee, M., Savin, S.M., 1985. Isolation of diagenetic overgrowths on sand grains for oxygen isotope analysis. *Geochim. Cosmochim. Acta* 49, 664–669.
- Longstaffe, F.J., 1989. Stable isotopes as tracers in clastic diagenesis. In: Hutcheon, I.E. (Ed.), *Short Course in Burial Diagenesis*. Short Course Ser.-Mineral. Assoc. Can., vol. 15, pp. 201–277.
- Lyon, I.C., Burley, S.D., McKeever, P.J., Saxton, J.M., Macaulay, C., 2000. Oxygen isotope analysis of authigenic quartz in sandstones: a comparison of ion microprobe and conventional analytical techniques. In: Worden, R.H., Morad, S. (Eds.), *Quartz Cementation in Sandstones*. Int. Assoc. Sedimentol., Spec. Publ., vol. 29, pp. 299–316.
- Macaulay, C.I., Boyce, A.J., Fallick, A.E., Haszeldine, R.S., 1997. Quartz veins record vertical flow at a graben edge: Fulmar Oil Field, central North Sea. *AAPG Bull.* 81, 2024–2035.
- Macaulay, C.I., Fallick, A.E., Haszeldine, R.S., Graham, C.M., 2000. Methods of laser-based stable isotope measurement applied to diagenetic cements and hydrocarbon reservoir quality. *Clay Miner.* 35, 313–322.
- Marchand, A.M.E., 2001. Diagenesis and porosity preservation in deepwater oilfield sandstones. PhD thesis, The University of Edinburgh, pp. 231.
- Marchand, A.M.E., Haszeldine, R.S., Macaulay, C.I., Swennen, R., Fallick, A.E., 2000. Quartz cementation inhibited by cretal oil charge: Miller deep water sandstone, UK North Sea. *Clay Miner.* 35, 205–214.
- Marchand, A.M.E., Haszeldine, R.S., Smalley, P.C., Macaulay, C.I., Fallick, A.E., 2001. Evidence for reduced quartz-cementation rates in oil-filled sandstones. *Geology* 29, 915–918.
- Marchand, A.M.E., Smalley, P.C., Haszeldine, R.S., Fallick, A.E., 2002. Note on the importance of hydrocarbon-fill for reservoir quality prediction in sandstones. *AAPG Bull.* 86, in press.
- Matsuhisa, Y., Goldsmith, J.R., Clayton, R.N., 1979. Oxygen isotopic fractionation in the system quartz–albite–anorthite–water. *Geochim. Cosmochim. Acta* 43, 1131–1140.
- McBride, E.F., 1989. Quartz cement in sandstones: a review. *Earth-Sci. Rev.* 26, 69–112.
- McClure, N.M., Brown, A.A., 1990. Miller Field: a subtle Upper Jurassic submarine fan trap in the South Viking Graben, UK Sector North Sea. In: Halburty, M.T. (Ed.), *Giant Oil and Gas Fields of the Decade 1978–1988*. AAPG Mem., vol. 54, pp. 307–322.
- McLaughlin, O.M., Haszeldine, R.S., Fallick, A.E., 1996. Quartz diagenesis in layered fluids in the South Brae oilfield, North Sea. *Soc. Econ. Paleontol. Mineral. Spec. Publ.* 55, 103–113.
- Milliken, K.L., Land, L.S., Loucks, R.G., 1981. History of burial diagenesis determined from isotopic geochemistry, Frio Formation, Brazoria County, Texas. *AAPG Bull.* 65, 1397–1413.
- Paxton, S.T., Szabo, J.O., Calvert, C.S., Ajdukiewicz, J.M., 1990. Preservation of primary porosity in deeply buried sandstones: a new play concept from the Cretaceous Tuscaloosa Sandstone of Louisiana (Abs.). *AAPG Bull.* 74, 737.
- Rooksby, S.K., 1991. The Miller Field, Blocks 16/7b, 16/8b, UK North Sea. In: Abbotts, I.L. (Ed.), *United Kingdom Oil and Gas Fields, 25 Years Commemorative Volume*. Geological Society London Memoir, vol. 14, pp. 159–164.
- Saigal, G.C., Bjørlykke, K., 1987. Carbonate cements in clastic reservoir rocks from offshore Norway—relationships between isotopic composition, textural developments and burial depth. In: Marshall, J.D. (Ed.), *Diagenesis of Sedimentary Sequences*. Spec. Publ.-Geol. Soc. London, vol. 36, pp. 313–324.
- Smalley, P.C., Warren, E.A., 1994. The Miller Field. In: Warren, E.A., Smalley, P.C. (Eds.), *North Sea Formation Water Atlas*. Geological Society London Memoir, vol. 15, p. 52.
- Sullivan, K.B., McBride, E.F., 1991. Diagenesis of sandstones at shale contacts and diagenetic heterogeneity, Frio Formation, Texas. *AAPG Bull.* 75, 121–138.
- Valley, J.W., Graham, C.M., 1996. Ion microprobe analysis of oxygen isotope ratios in quartz from Skye granite: healed microcracks, fluid flow, and hydrothermal exchange. *Contrib. Mineral. Petrol.* 124, 225–234.
- Walderhaug, O., 1994. Temperatures of quartz cementation in Jurassic sandstones from the Norwegian continental shelf—evi-

- dence from fluid inclusions. *J. Sediment. Res., Sect. A Sediment. Pet. Proc.* 64, 311–323.
- Wilkinson, M., Crowley, S.F., Marshall, J.D., 1992. Model for the evolution of oxygen isotope ratios in the pore fluids of mudrocks during burial. *Mar. Pet. Geol.* 9, 98–105.
- Williams, L.B., Hervig, R.L., Bjørlykke, K., 1997. New evidence for the origin of quartz cements in hydrocarbon reservoirs revealed by oxygen isotope microanalyses. *Geochim. Cosmochim. Acta* 61, 2529–2538.